

Effect of Design and Heat Treatment on the Mechanical Properties of NiTi Rotary Instruments

Seok Woo Chang^{1,2*}, Soram Oh^{1,2}, Hyun-Jung Kim², Bong-Ki Jeon³, Kee-Yeon Kum⁴, Hiran Perinpanayagam⁵

¹Department of Conservative Dentistry, Kyung Hee university, Seoul, Republic of Korea

²Department of Conservative Dentistry, Kyung Hee University, Seoul, Republic of Korea

³Ilsanstar 28 Dental Clinic, Goyang, Republic of Korea

⁴Department of Conservative Dentistry, Seoul National University, Seoul National University, Seoul, Republic of Korea

⁵ Department of Dentistry, University of Western Ontario, London, UK

Research Article

Received: 12-Sep-2022, Manuscript

No, JDS-22-71772;

Editor assigned: 15-Sep-2022,

Manuscript No, JDS-22-71772 (PQ);

Reviewed: 29-Sep-2022, QC No.

JDS-22-71772;

Revised: 06-Oct-2022, QC No. JDS-

22-71772

Published:- 12-Oct-2022,

DOI:10.4172/2320-7949.10.6.001

***For Correspondence:**

Seok Woo Chang, Department of Conservative Dentistry, Kyung Hee University Dental Hospital, Seoul, Republic of Korea

E-mail: swc2007smc@khu.ac.kr

Keywords: Differential scanning calorimetry; Heat treatment; Mechanical properties; Nickel-titanium rotary instrument

ABSTRACT

Adult Background/purpose: NiTi files have been manufactured with various designs and heat treatments. This study aimed to determine the effects of design and heat treatment on the mechanical properties of NiTi instruments. **Materials and methods:** ProFile, Profa File Gold, ProTaper Universal, ProTaper Gold, Profa Taper Gold, and ExactTaper H (n=44/brand) were subjected to bending, buckling, cyclic fatigue and torsional resistance tests (n=10/brand/test). Instrument surfaces were examined with scanning electron microscopy (SEM) (n=2/brand), and phase transformation behavior studied by differential scanning calorimetry (DSC) (n=2).

Results: ProFile and Profa File Gold showed a concave triangular cross-section with radial lands, while other NiTi files had a convex triangular cross-sectional design. DSC curves revealed that austenitic transformation-finishing temperature of Profa File Gold, ProTaper Gold, Profa Taper Gold and ExactTaper H were above 37°C. ProTaper Universal, Profa Taper Gold, and ExactTaper H presented the highest bending resistance. ProTaper Universal showed the highest buckling resistance, elastic modulus, and the lowest cyclic fatigue resistance. ExactTaper H exhibited the highest cyclic fatigue resistance and ultimate torsional strength. ProTaper Gold and ExactTaper H showed the greatest angle of rotation until fracture and consisted of mainly R-phase at room temperature.

Conclusion: NiTi instrument's mechanical properties were affected significantly by both design and heat treatment.

INTRODUCTION

Nickel-Titanium Rotary Instruments (NiTi files) have enabled faster root canal shaping and better centering ability in curved canals compared to hand instrumentation [1]. There have been advancements in the manufacturing of NiTi rotary instruments, including geometric shape variation, thermomechanical treatments, and altered kinematic movements to increase cutting efficiencies and reduce fractures [2-5]. ProFile (Dentsply Sirona, Maillefer, Ballaigues, Switzerland) comprises three U-shaped flutes with three radial lands [6]. Their U-shaped flute and negative rake angle enable cutting root dentin equally over 360° and superior centering ability [7]. While ProFile has a constant taper, ProTaper Universal files have variable taper within an instrument. ProTaper Universal shaping files (S1, S2) have progressive taper, and finishing files (F1, F2, F3) have regressive taper [8]. Their variable taper design reduces the screw-in effect of the rotary instrument [9]. Recently, various kinds of heat-treated NiTi files have been manufactured [10]. According to Differential Scanning Calorimetric (DSC) analysis, phase transformation temperatures of heat-treated files are different from those of conventional NiTi files and a certain amount of R-phase and/or martensite are present at room temperature [11,12]. ProTaper Gold (Dentsply Sirona) files that have identical geometric design to ProTaper Universal are manufactured by heat treatment to have a golden-colored surface [13]. ProTaper Gold files exhibit less transportation in canal curvatures than ProTaper Universal due to enhanced flexibility [14]. Exact Taper™ H (SS White Dental, Lakewood, NJ, USA) files manufactured through heat treatment have multiple tapers within an instrument, similar to the ProTaper series. Profa File Gold (Profa, Shenzhen Perfect medical instruments, Shanwei, China) and Profa Taper Gold (Profa, Shenzhen Perfect medical instruments), made through heat treatment, are replica-like products with the same design as ProFile and ProTaper Gold, respectively. However, no studies have reported on the mechanical properties of Exact Taper™ H, Profa File Gold, or Profa Taper Gold. The objective of this study was to evaluate the mechanical properties of ProFile, Profa File Gold, ProTaper Universal, ProTaper Gold, Profa Taper Gold, and ExactTaper H, which were fabricated with various designs and heat treatments. Their bending, buckling, cyclic fatigue, torsional resistance, and phase transformation behaviors were studied. The null hypotheses tested were that NiTi rotary instruments' mechanical properties are not affected by i) instrument design and ii) heat treatment.

MATERIALS AND METHODS

ProFile, Profa File Gold, ProTaper Universal, ProTaper Gold, Profa Taper Gold, and ExactTaper H instruments (n=44/brand) were used (Table 1). All instruments were ISO size #25 and length 21 mm. ProFile and Profa File Gold have a constant 6% taper with concave triangular cross-sectional designs, whereas ProTaper Universal, ProTaper Gold, Profa Taper Gold, and ExactTaper H have variable tapers with convex triangular cross-sectional designs. ProFile and ProTaper Universal are manufactured without heat treatment, while Profa File Gold, ProTaper Gold, Profa Taper Gold, and ExactTaper H are made using heat treatment. Instruments were subjected to four mechanical tests (n=10/brand/test), which were bending, buckling, cyclic fatigue, and torsional resistance tests using a universal testing machine (UTM; Universal Mechanics Analyzer, IB Systems, Seoul, Korea).

Table 1. Specifications for NiTi rotary instruments studied.

Product	Tip size, taper	Cross-section	Alloy type	Manufacturer
ProFile	#25/06, constant taper	Three U-shaped flutes with radial land	Conventional	Denstply Sirona, Maillefer, Ballaigues, Switzerland
Profa File Gold	#25/06, constant taper	Three U-shaped flutes with radial land	Gold wire	Profa, Shenzhen Perfect medical instruments, Shanwei, China
ProTaper Universal	F2 (#25, variable taper)	Convex triangle	Conventional	Denstply Sirona
ProTaper Gold	F2 (#25, variable taper)	Convex triangle	Gold wire	Denstply Sirona
Profa Taper Gold	F2 (#25, variable taper)	Convex triangle	Gold wire	Profa, Shenzhen Perfect medical instruments,
ExactTaper H	F2 (#25, variable taper)	Convex triangle	Blue wire	SS White, Lakewood, CA, USA

Bending resistance test

Based on ISO3630-1:2019, the apical 3 mm tip of the file was tightly clamped into a chuck that was connected to the load cell of UTM. The file tip was bent at a speed of 2 rpm using a rotating pin located at 10 mm from the chuck. The bending resistance (N cm) was recorded as the torque when the file was bent 45°.

Buckling resistance test

A customized cube block (IPS e.max CAD; Ivoclar Vivadent, Schaan, Liechtenstein) with a small dimple was used. The file tip was in contact with the cube block while the handle was fixed to the upper part of UTM. The file was moved in the axial direction of the instrument at a crosshead speed of 1.2 mm/s, while the file tip was restrained in a small dimple. The axial load was measured during the instrument deflection, and the buckling resistance (gf) was recorded as the maximum load during the 1-mm axial movement of the file.

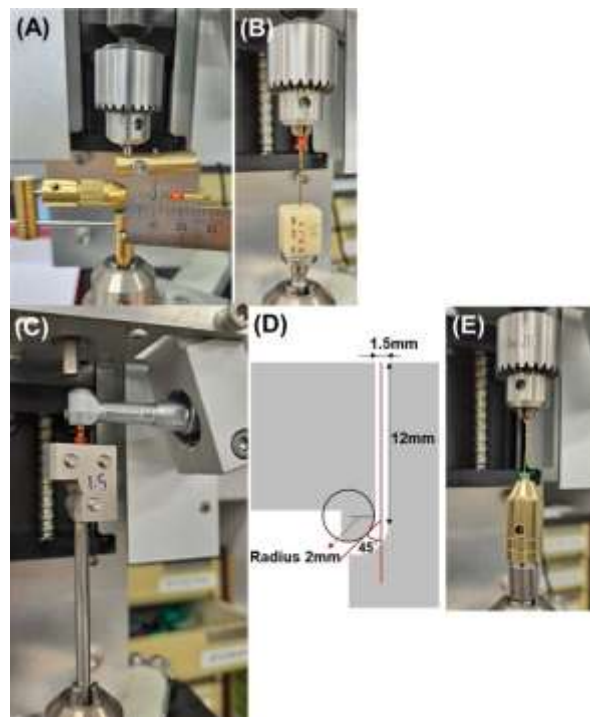
Cyclic fatigue resistance test

A customized jig with an artificial metallic curved canal was used. The artificial metallic canal had a diameter of 1.5 mm, a curvature with an inner radius of 2 mm, and a 45° angle. The NiTi file was operated with X-Smart motor (Dentsply Sirona, Ballaigues, Switzerland) at 300 rpm. The time was recorded in seconds until the fracture of the file.

Torsional resistance test

Based on ISO3630-1:2019, the apical 3 mm tip of the file was tightly clamped into a chuck that was connected to the load cell of the UTM. Then, the shaft of the instrument was fastened to an opposing chuck that could be rotated. The file was rotated in the clockwise direction at 2 rpm until fracture. The Angle of Rotation until Fracture (ARF) and Ultimate Torsional Strength (UTS) were obtained and a graph was plotted based on ARF and UTS. The Elastic Modulus (EM) was obtained from the slope on the linear portion of the torsional fracture resistance curve. (Figures 1 A-E)

Figure 1. The setups used for mechanical tests. A. bending resistance; B. buckling resistance; C. cyclic fatigue resistance; D. stainless-steel canal used in cyclic fatigue resistance tests; E. torsional fracture resistance.



Scanning electron microscopy

After cyclic fatigue and torsional fracture resistance tests, the fractured instruments were examined by Field Emission Scanning Electron Microscopy (FE-SEM) (JSM-7800F Prime; JEOL Ltd., Akishima, Tokyo, Japan) to identify the fracture mode. Additionally, lateral surfaces of new unused instruments were examined by FE-SEM ($n=2/\text{brand}$) (S-4700, Hitachi, Tokyo, Japan).

Statistical analysis

The normal distribution of data and the homogeneity of variances were verified by the Shapiro–Wilk test and Levene’s test, respectively. Bending, buckling resistances, fracture time from cyclic fatigue resistance test, ARF, UTS, and EM were compared by one-way Analysis of Variance (ANOVA) and Tukey’s post-hoc test using SPSS Statistics version 25 (IBM, Armonk, NY, USA) at a 95% significance level. Pearson correlation analysis was conducted between the six variables of the four mechanical test results. Two-way ANOVA was performed to evaluate the effect of instrument design, heat treatment, and their combined effects on the mechanical test results.

Differential scanning calorimetry

DSC was performed on new unused instruments ($n=2/\text{brand}$) to analyze phase-transformation behaviors by using DSC250 (TA Instruments, New Castle, DE, USA). The specimen was heated from 25 °C to 90 °C, then cooled to -90 °C, and then heated again to 90 °C at a rate of 10 °C/min. Enthalpy changes and phase transformation temperatures were measured during the heating and cooling cycles.

RESULTS

Bending resistance

The bending resistance of ProTaper Universal, Profa Taper Gold, and ExactTaper H were the highest ($p < 0.05$), followed by those of ProTaper Gold and ProFile. Profa File Gold showed the lowest bending resistance ($p < 0.05$).

Buckling resistance

ProTaper Universal had the highest buckling resistance, followed by Profa Taper Gold and ProTaper Gold ($p < 0.05$). ProFile, Profa File Gold, and Exact Taper H had lower buckling resistance ($p < 0.05$).

Cyclic fatigue resistance

ExactTaper H had the highest cyclic fatigue resistance with the longest fracture time, followed by Profa File Gold and ProTaper Gold ($p < 0.05$). ProFile and Profa Taper Gold demonstrated shorter fracture times than Profa File Gold and ProTaper Gold ($p < 0.05$). ProTaper Universal showed the least cyclic fatigue fracture resistance ($p < 0.05$).

Torsional resistance

ProTaper Gold and ExactTaper H demonstrated the greatest ARF ($p < 0.05$), followed by ProFile and Profa Taper Gold. ExactTaper H showed the highest UTS ($p < 0.05$), followed by Profa Taper Gold, ProTaper Gold and ProTaper Universal. ProFile and Profa File Gold presented the lowest UTS ($p < 0.05$). A representative UTS-ARF graph of each NiTi file was plotted in Figure 3. The slope on the linear portion of the graph was EM. ProTaper Universal had the highest EM, followed by Profa Taper Gold and Profa File Gold ($p < 0.05$). Pearson correlation analysis results among the six variables of mechanical tests were presented in Table 3. There was a strong positive relationship between the bending resistance and UTS ($p < 0.001$, Pearson's $r = 0.767$) and between the buckling resistance and EM ($p < 0.001$, Pearson's $r = 0.678$). A moderate negative relationship was observed between the buckling and cyclic fatigue resistances ($p < 0.001$, Pearson's $r = -0.591$) and between the cyclic fatigue resistance and EM ($p < 0.001$, Pearson's $r = -0.589$). Two-way ANOVA revealed that the effect of design and heat treatment on the six variables of mechanical test results were all statistically significant. The interaction of design and heat treatment significantly influenced buckling resistance, fracture time, ARF, and EM. (Tables 2 and 4 Figures 2 A-2F)

Figure 2. Mechanical testing results for each instrument. A. Bending resistance (N cm); B. Buckling resistance (gf); C. Cyclic fatigue resistance (fracture time in seconds); D. Angle of rotation until fracture from torsional resistance test (degrees); E. Ultimate torsional strength from torsional resistance test (N cm); F. Elastic modulus from torsional resistance test (N cm/degrees).

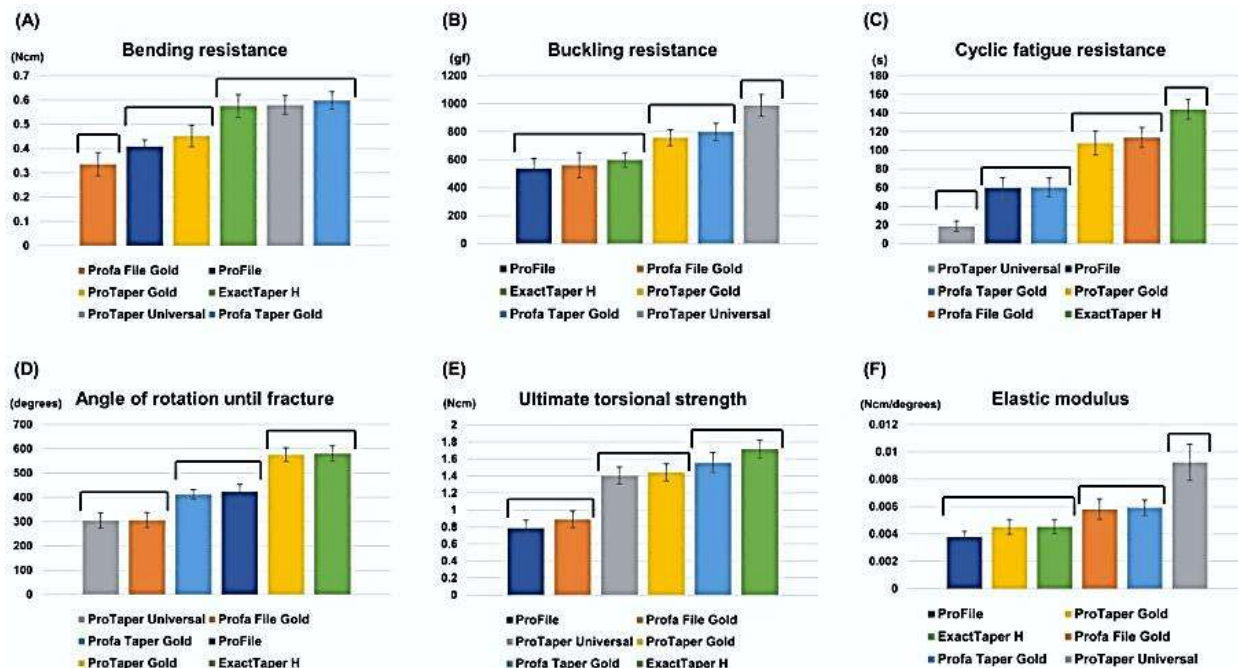


Figure 3. Representative graphs of ultimate torsional strength (UTS, Ncm) to angle of rotation (ARF, degrees) from torsional resistance tests of each instrument.

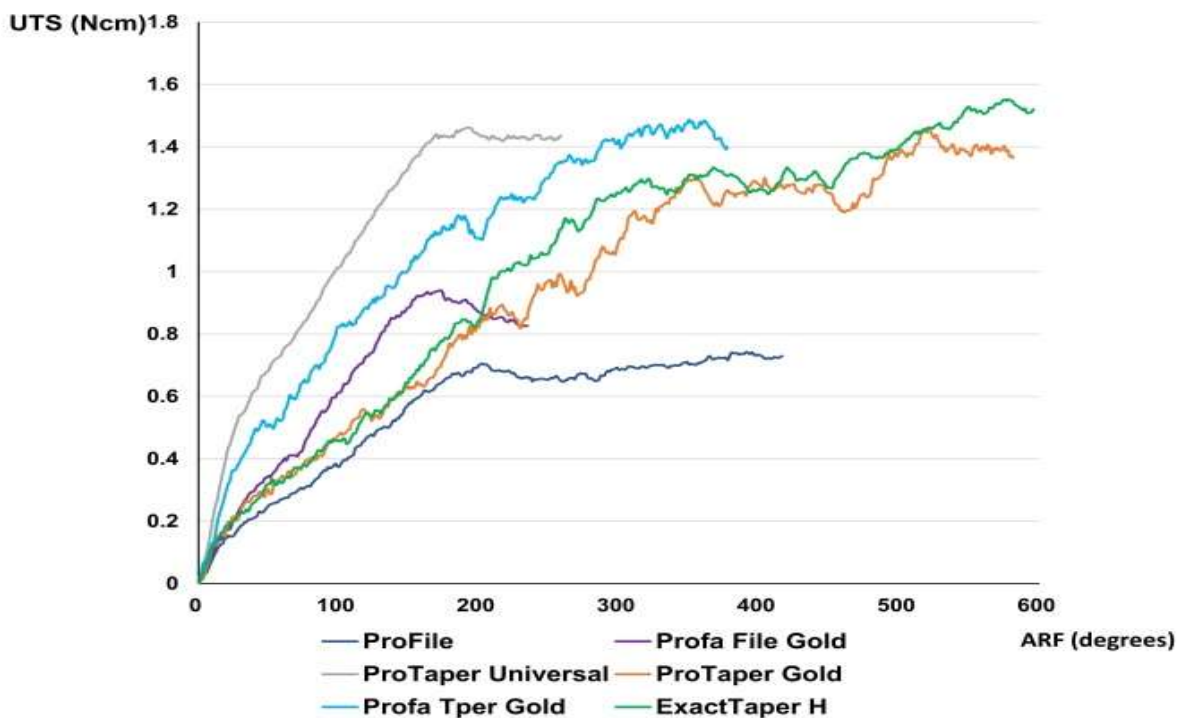


Table 2. Mechanical test results of NiTi files. Mean values (standard deviation)

Product	ProFile	Profa File Gold	ProTaper Universal	ProTaper Gold	Profa Taper Gold	Exact Taper H
Bending resistance (Ncm)	0.409 (0.026) ^b	0.335 (0.047) ^a	0.579 (0.039) ^c	0.452 (0.045) ^b	0.598 (0.036) ^c	0.576 (0.047) ^c
Buckling resistance (gf)	537.721 (73.006) ^a	560.641 (88.976) ^a	987.676 (78.913) ^c	757.672 (57.313) ^b	798.963 (62.154) ^b	597.966 (51.911) ^a
Fracture time (s)	59.71 (10.96) ^b	113.74 (10.57) ^c	18.59	107.88 (12.79) ^c	60.23 (10.06) ^b	144.01 (10.73) ^d
ARF (degrees)	423.47 (29.77) ^b	305.83 (31.10) ^a	304.55 (31.92) ^a	575.77 (27.99) ^c	412.58 (19.63) ^b	580.98 (31.99) ^c
UTS (Ncm)	0.786 (0.092) ^a	0.891 (0.100) ^a	1.405 (0.099) ^b	1.442 (0.099) ^b	1.557 (0.116) ^{b,c}	1.717 (0.106) ^d
EM (Ncm/degrees)	0.0038 (0.0004) ^a	0.0058 (0.0008) ^b	0.0092 (0.0013) ^c	0.0045 (0.0005) ^a	0.0059 (0.0006) ^b	0.0045 (0.0005) ^a
<p>Note: ARF: Angle of Rotation until Fracture; UTS: Ultimate Torsional Strength; EM: Elastic Modulus Different superscript letters in each row indicate significant difference between groups.</p>						

Scanning electron microscopy

Instruments fractured by cyclic fatigue tests presented typical patterns of dimples and multiple fatigue striations on their fractured surface. The lateral surface showed a brittle fracture pattern without plastic deformation, and multiple cracks were observed near the fractured plane. Instruments fractured by torsional tests showed concentric circular abrasion marks and skewed fibrous dimples near the center of rotation. The lateral part of the fractured instrument showed a ductile fracture pattern with a torn-off appearance. Lateral surfaces of unused instruments revealed that ProFile and Profa File Gold had nearly identical designs with radial lands. ProTaper Universal, ProTaper Gold, Profa Taper Gold, and ExactTaper H had similar designs, demonstrating variable taper and increased pitch length along the shaft. Pitch lengths for ProTaper Universal, ProTaper Gold, Profa Taper Gold, and ExactTaper H were longer than those of ProFile and Profa File Gold (Figures 4A-4C, 5A-5C and 6A-6F).

Table 3. Pearson correlation analysis result.

		Pearson correlation analysis	
		coefficient	p-value
Bending resistance	Buckling resistance	0.572*	<0.001
	Fracture time	-0.251	0.053
	Angle of rotation until fracture	0.198	0.13
	Ultimate torsional strength	0.767*	<0.001
	Elastic modulus	0.337*	0.008
Buckling resistance	Fracture time	-0.591*	<0.001
	Angle of rotation until fracture	-0.212	0.103
	Ultimate torsional strength	0.431*	0.001
	Elastic modulus	0.678*	<0.001
Fracture time	Angle of rotation until fracture	0.596*	<0.001
	Ultimate torsional strength	0.173	0.186
	Elastic modulus	-0.589*	<0.001
Angle of rotation until fracture	Ultimate torsional strength	0.472*	<0.001

Note: An asterisk means a significant linear relationship between two variables.

Table 4. Result of two-way of Analysis of Variance.

	Bending resistance	Buckling resistance	Fracture time	Angle of rotation until fracture	Ultimate torsional strength	Elastic modulus
Design	<0.001*	<0.001*	0.002*	0.010*	<0.001*	<0.001*
Heat treatment	0.003*	<0.001*	<0.001*	0.008*	0.001*	<0.001*
Design x heat treatment	0.319	<0.001*	0.049*	<0.001*	0.418	<0.001*

Note: P values from two-way Analysis of Variance are presented. An asterisk indicates statistically significant effect (p<0.05).

Figure 4. Scanning electron microscopic images of fractured specimens from cyclic fatigue resistance test. A. fractured surface; B. magnified views of the arrow in A; C. lateral surface of fractured instruments, arrows indicate cracks. From left to right, ProFile, Profa File Gold, ProTaper Universal, ProTaper Gold, Profa Taper Gold, and ExactTaper H.

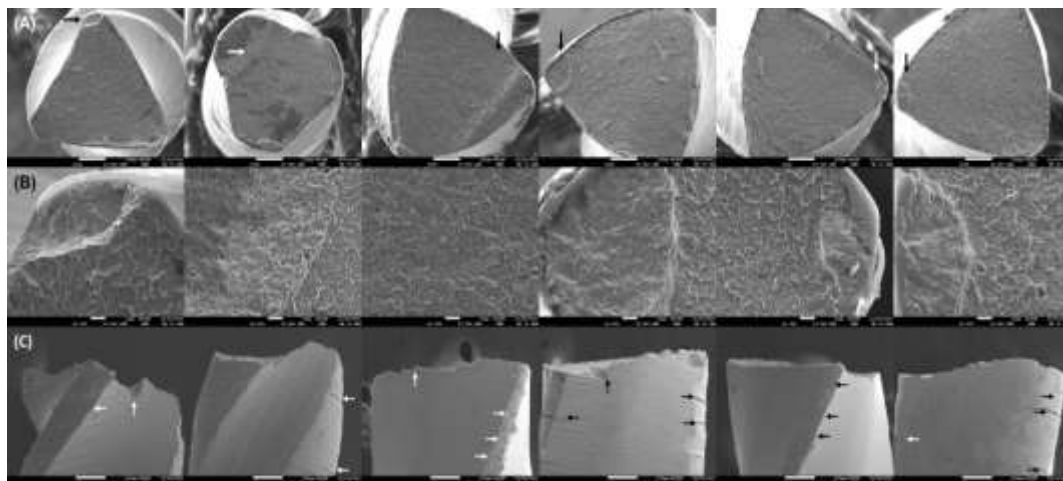


Figure 5. Scanning electron microscopic images of fractured specimens from torsional resistance test. A. fractured surface; B. magnified views of arrow in a; C. lateral surface of fractured instruments. From left to right, ProFile, Profa File Gold, ProTaper Universal, ProTaper Gold, Profa Taper Gold, and ExactTaper H.

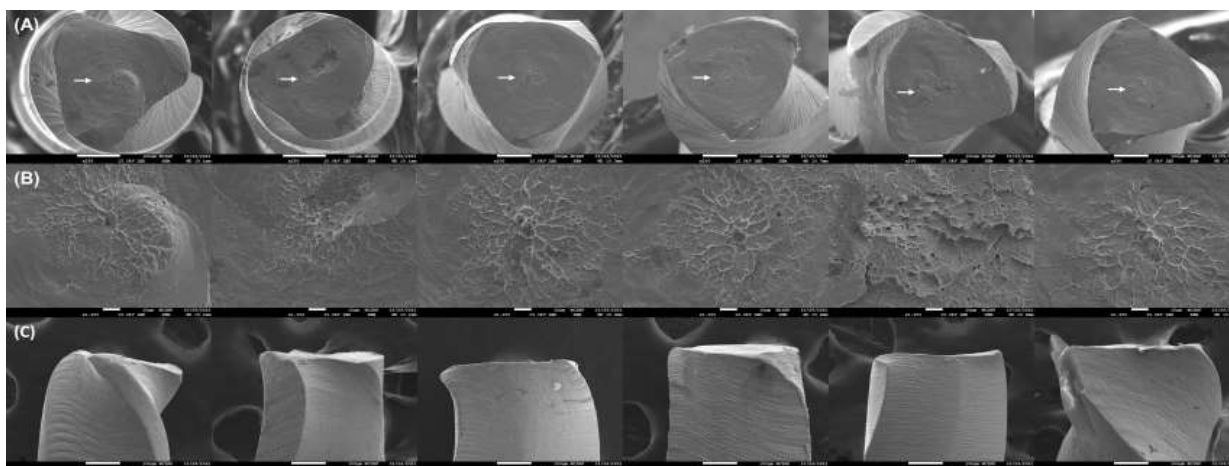
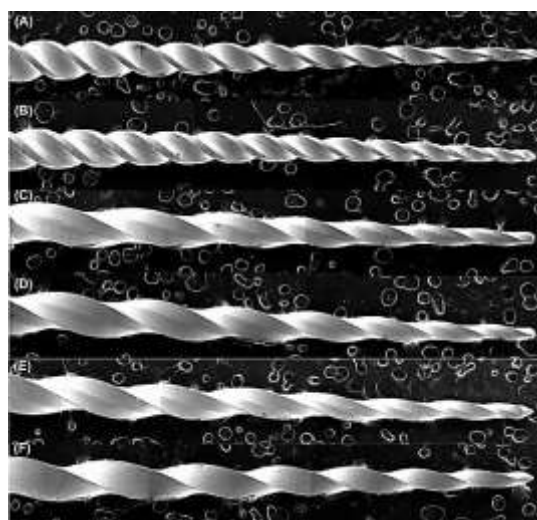


Figure 6. Scanning electron microscopic images of lateral surfaces of new unused ProFile; A. Profa File Gold B. ProTaper Universal; C. ProTaper Gold; D. Profa Taper Gold ;E. ExactTaper H F.



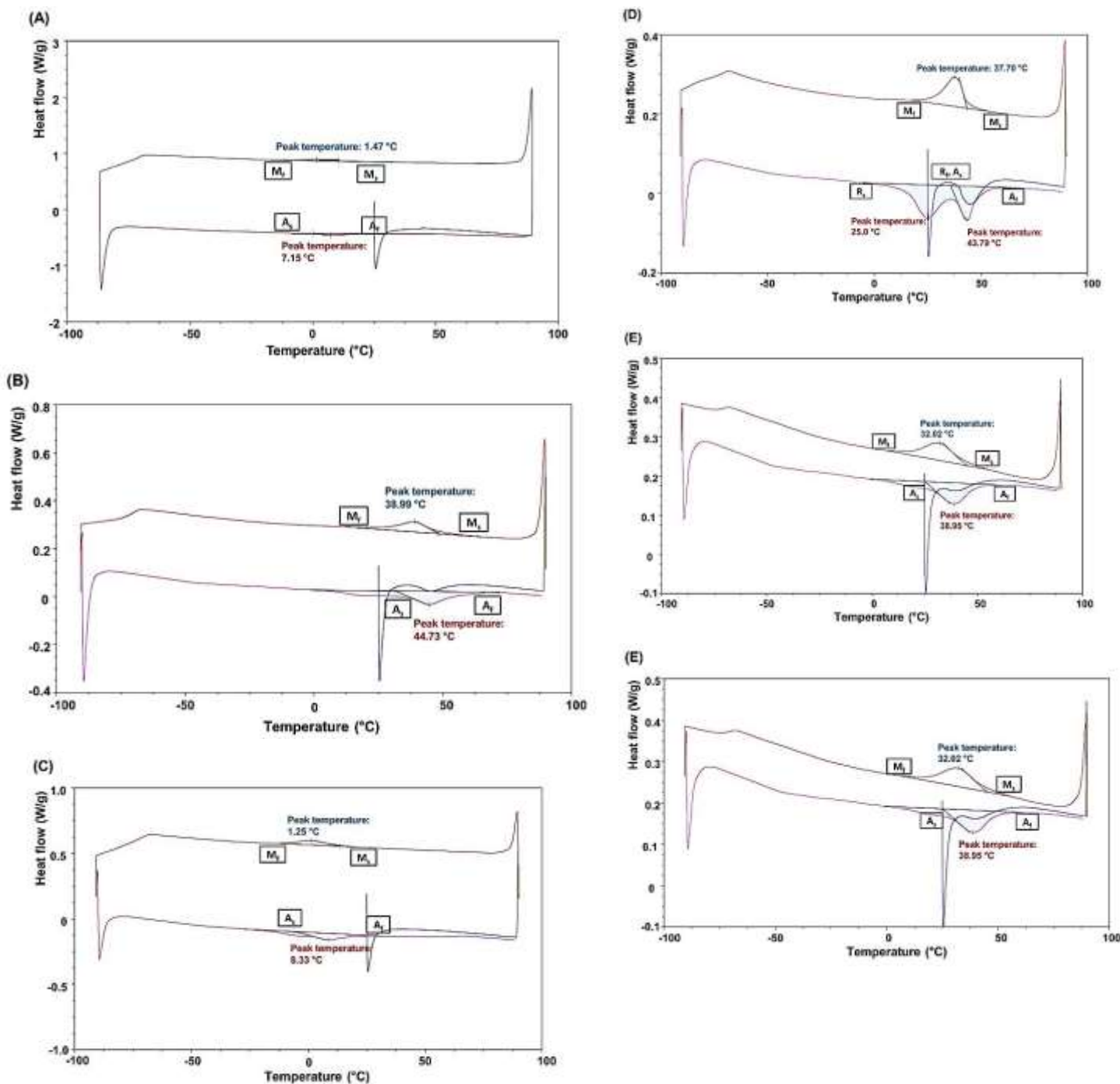
Differential scanning calorimetry

The DSC plots of Pro File and Pro Taper Universal showed a single peak in the heating and cooling curves, and both peaks were observed below room temperature. The DSC plots of Profa File Gold and Profa Taper Gold showed a single peak in the heating and cooling curves, and both peaks were observed above room temperature. The DSC plot of Pro Taper Gold exhibited two successive peaks in the heating curve, a single peak in the cooling curve, and all peaks were above room temperature. The DSC plot of Exact Taper H showed a peak in the heating curve and two separated peaks in the cooling curve. The peak in the heating curve of Exact Taper H was observed above room temperature. Table 5 summarizes the transformation temperature and associated energy of all the files (Figures 7A-7F).

Table 5. Transformation temperatures and associated energy from the DSC plots of tested NiTi files.

	Cooling						Heating		
	Rs(°C)	Rf(°C)	ΔH (J/g)	Ms(°C)	Mf(°C)	ΔH (J/g)	As(°C)	Af(°C)	ΔH (J/g)
ProFile				10.7	-6.25	1.78	0.42	14.38	2.47
Profa File Gold				48.6	28.3	4.04	31.5	61.51	8.36
ProTaper Universal				13.4	-9.82	3.1	8.33	22.32	7.05
ProTaper Gold				43.5	25.9	5.06	35.9	52.68	12.5
Profa Taper Gold				44.8	16.3	4.9	25	50	6.6
ExactTaper H	38.43	28.1	4.15	-29.02	-63.28	4.88	23.1	43.75	13.88

Figure 7. DSC plots of ProFile. A. Profa File Gold; B. ProTaper Universal; C. ProTaper Gold; D. Profa Taper Gold; E. ExactTaper H; F. Lower and upper curves are heating and cooling curves, respectively. R_s and R_f , R-phase transformation-starting and finishing temperature; M_s and M_f , martensitic transformation-starting and finishing temperature; A_s and A_f , austenitic transformation-starting and finishing temperature.



DISCUSSION

NiTi files with convex triangular cross-sectional design and variable tapers showed higher bending, buckling resistances, and UTS than files with concave triangular cross-sections and constant tapers. Greater taper at the tip region and larger cross-sectional area contributed to higher bending resistance and UTS, which is consistent with previous studies^[15-17]. Buckling is defined as a sudden sideways deflection of the file, which occurs when the compressive load exceeds the instrument's resistance^[18]. Instruments with higher flexibility have less bending resistance, and tend to have lower buckling resistance^[19]. In this study, Pearson's correlation analysis showed a positive moderate to strong correlation between bending, buckling resistances, and UTS (Pearson's $r=0.431\sim0.767$). NiTi files with heat treatment showed lower bending and buckling resistances. The soft and ductile properties of martensite play an important role in preventing fracture of NiTi files^[20]. The martensitic phase also has excellent damping characteristics owing to the energy absorption abilities of its twinned phase structure^[21]. The NiTi files made using heat treatment, which possess martensite at room temperature, demonstrated superior resistance to cyclic fatigue and torsional fracture, which has also been reported in previous studies^[22,23]. Cyclic fatigue fracture occurs due to repetitive compressive and tensile stresses when the instrument rotates in a curved canal^[24]. Since repetitive bending stress is the cause of cyclic fatigue fracture of NiTi file, more flexible instruments can be more resistant to cyclic fatigue fracture^[12,20]. The flexibility of an instrument was assessed using the EM. The correlation between NCF and EM (Pearson's $r=-0.589$) implies that an instrument with higher flexibility (lower EM) was more resistant to cyclic fatigue fracture. Bending resistance is also related to flexibility. However, in this study, the correlation between bending and cyclic fatigue resistance was insignificant ($p=0.053$). In this study, cyclic fatigue resistance (fracture time) of NiTi files were affected by both design and heat treatment, and their interaction was significant. Although ProTaper Gold, Profa Taper Gold, and ExactTaper H showed identical designs and were manufactured through heat treatment, ExactTaper H and ProTaper Gold are composed of R-phase at room temperature, unlike Profa Taper Gold. The R-phase is a transitional phase between martensite and austenite with a rhombohedral structure that can be formed during conversion between austenite and martensite^[25]. The R-phase has a lower EM than martensite or austenite, and the transformation strain of the R-phase is less than 10% of that of the martensitic transformation^[26]. Therefore, presence of the R-phase may account for the superior cyclic fatigue resistance of ProTaper Gold and ExactTaper H compared to Profa Taper Gold. Among two conventional NiTi files, ProFile was more resistant to cyclic fatigue than ProTaper Universal owing to superior flexibility, supported by lower bending resistance and EM. Collectively, geometric designs and metallurgical properties influenced cyclic fatigue resistance. Torsional fracture resistance of NiTi rotary instruments involves two assessments. These are ARF that is related to "ductility," and UTS, which is related to "mechanical resistance"^[17,20]. The ductility of NiTi alloys is the ability to deform plastically without fracture when stress is applied. Heat-treated NiTi files had greater ARF than conventional NiTi files owing to the ductile nature of martensite, which is consistent with previous studies^[15,27]. NiTi files that are composed of R-phase demonstrated the highest ARF. NiTi files with convex triangular cross-sections had higher UTS than those with concave triangular cross-sections and radial lands. As the distance between the middle of each side of the triangle and the centroid is shorter than that of a convex triangle, the stress concentration may be higher in the middle of each side^[28,29]. ProTaper Universal demonstrated the highest EM, which indicated stiffness. Therefore, ProTaper Universal is not recommended for curved canals due to their risk of transportation^[14,30]. The heating curves of DSC plots indicated that conventional NiTi instruments, ProFile and ProTaper Universal, have the austenitic structure at 22°C. Profa File Gold has martensitic structure, Profa Taper

Gold has mixed structure of austenite and martensite at 22°C. ProTaper Gold has mixed state of martensite and R-phase, while ExactTaper H has mixed state of austenite, martensite and R-phase at 22°C. Heat treatment resulted in the phase composition of NiTi instrument, which affected mechanical properties such as bending, cyclic fatigue, and torsional resistances. (Figures 2A-2D and 7A-7F)

CONCLUSION

In conclusion, the mechanical properties of NiTi rotary files varied significantly with the design and heat treatment of the instruments ($p < 0.05$). NiTi files with a convex triangular cross-section and a longer pitch length showed higher bending and buckling resistances, and ultimate torsional strength. NiTi files manufactured using heat treatment demonstrated superior resistance to cyclic fatigue.

DECLARATION OF COMPETING INTEREST

The authors have no conflicts of interest relevant to this study.

ACKNOWLEDGEMENTS

This work was supported by a grant from Kyung Hee University in 2021 (KHU-20210146), and by a grant from the National Research Foundation of Korea (MIST No. 2021R1F1A1045987).

REFERENCES

1. Paleker F, et al. Comparison of canal transportation and centering ability of K-files, ProGlider file, and G-files: a micro-computed tomography study of curved root canals. *J Endod.* 2010; 42:1105-1159.
2. Conceição I, et al. Simulated root canals preparation time, comparing ProTaper next and waveOne Gold systems, performed by an undergraduate student. *J Clin Exp Dent.* 2020;12:e730-e735.
3. Van der Vyver PJ, et al. Root canal shaping using nickel titanium, M-wire, and gold wire: a micro-computed tomographic comparative study of One Shape, ProTaper Next, and WaveOne Gold instruments in maxillary first molars. *J Endod.* 2019;45:62-67.
4. Shi L, et al. Shaping ability of ProTaper Gold and WaveOne Gold nickel-titanium rotary instruments in simulated S-shaped root canals. *J Dent Sci.* 2022;17:430-437
5. Chi CW, et al. Influence of heat treatment on cyclic fatigue and cutting efficiency of ProTaper Universal F2 instruments. *J Dent Sci.* 2017;12:21-26.
6. Hsu YY, et al. The ProFile system. *Dent Clin North Am.* 2004;48:69-85.
7. Al-Sudani D, et al. A comparison of the canal centering ability of ProFile, K3, and RaCe nickel titanium rotary systems. *J Endod.* 2006;32:1198-1201.
8. Clauder T, et al. ProTaper NT system. *Dent Clin North Am.* 2004;48:87-111.
9. Iqbal MK, et al. Comparison of apical transportation between ProFile and ProTaper NiTi rotary instruments. *Int Endod J.* 2004;37:359-364.
10. Tabassum S, et al. Nickel-titanium rotary file systems: What's new?. *Eur Endod J.* 2019;4:111-117.
11. Zupanc J, et al. New thermomechanically treated NiTi alloys: a review. *Int Endod J.* 2018;51:1088-1003.
12. Oh S, et al. Bending resistance and cyclic fatigue resistance of waveone gold, reciproc blue, and hyFlex EDM instruments. *J Dent Sci.* 2020;15:472-478.

13. Plotino G, et al. Influence of temperature on cyclic fatigue resistance of protaper gold and protaper Universal rotary files. *J Endod.* 2017;43:200-202.
14. Silva EJ, et al. Comparison of canal transportation in simulated curved canals prepared with ProTaper Universal and ProTaper Gold systems. *Restor Dent Endod.* 2016;41:1-5.
15. Ninan E, et al. Torsion and bending properties of shape memory and superelastic nickel-titanium rotary instruments. *J Endod.* 2013;39:101-104.
16. Ha JH, et al. Geometric optimization for development of glide path preparation nickel-titanium rotary instrument. *J Endod.* 2015;41:916-919.
17. Alqedairi A, et al. Torsional resistance of three ProTaper rotary systems. *BMC Oral Health.* 2019;19:124.
18. Lopes HP, et al. Mechanical behavior of pathfinding endodontic instruments. *J Endod.* 2012;38:1417-1421.
19. Lopes WSP, et al. Bending, buckling and torsional resistance of rotary and reciprocating glide path instruments. *Int Endod J.* 2020;53:1689-1695.
20. Shim KS, et al. Mechanical and metallurgical properties of various nickel-titanium rotary instruments. *Biomed Res Int.* 2017;2017:452-601.
21. . Shen Y, et al. Metallurgical characterization of controlled memory wire nickel-titanium rotary instruments. *J Endod.* 2011;37:1566-1571.
22. Kaval ME, et al. Evaluation of the cyclic fatigue and torsional resistance of novel nickel-titanium rotary files with various alloy properties. *J Endod.* 2016;42:1840-1843.
23. Plotino G, et al. Influence of temperature on cyclic fatigue resistance of protaper Gold and protaper Universal rotary files. *J Endod.*2017;43:200-202.
24. Whipple SJ, et al. Cyclic fatigue resistance of two variable-taper rotary file systems: protaper universal and v-taper. *J Endod.* 2009;35:555-558.
25. Duerig TW, et al. The Influence of the R-Phase on the superelastic behavior of niti. *Shape Mem Superelasticity.* 2015;1:153-161.
26. Wu SK, et al. A study of electrical resistivity, internal friction and shear modulus on an aged ti49Ni51 alloy. *Acta Metallurgica et Materialia.* 1990;38:95-102.
27. Goo H-J, et al. Mechanical properties of various heat-treated nickel-titanium rotary instruments. *J Endod.* 2017;43:1872-1877.
28. Park SY, et al. Dynamic torsional resistance of nickel-titanium rotary instruments. *J Endod.* 2010;36:1200-1204.
29. Xu X, et al. Comparative study of torsional and bending properties for six models of nickel-titanium root canal instruments with different cross-sections. *J Endod.* 2006;32:372-375.
30. Silva EJ, et al. Quantitative transportation assessment in simulated curved canals prepared with an adaptive movement system. *J Endod.* 2015;41:1125-1129.